

## Electronic Supplementary Information

### **Cooperative self-assembling process of core-substituted naphthalenediimide induced by amino-yne click reaction**

Minghan Tan,<sup>ab</sup> Masayuki Takeuchi<sup>\*ab</sup> and Atsuro Takai<sup>\*a</sup>

<sup>a</sup> Molecular Design and Function Group, National Institute for Materials Science (NIMS),  
1-2-1 Sengen, Tsukuba, Ibaraki 305-0047, Japan

<sup>b</sup> Department of Materials Science and Engineering, Faculty of Pure and Applied Sciences,  
University of Tsukuba, 1-1-1 Tennodai, Tsukuba, Ibaraki 305-8577, Japan

## Table of Contents

S1. Experimental Methods	Page S1
S2. Synthesis and Characterization	Page S3
S3. Spectral Analyses	Page S7
S4. Supporting Data (Fig. S1–S13 and Table S1, S2)	Page S8
S5. Supporting References	Page S22

### S1. Experimental Methods

#### Abbreviations of Chemical Names:

CHCl <sub>3</sub>	chloroform
CDCl <sub>3</sub>	chloroform- <i>d</i>
MCH	methylcyclohexane
THF	tetrahydrofuran
TMS	tetramethylsilane

**Materials:** Unless otherwise noted, all reagents and solvents were purchased from Tokyo Chemical Industry, Sigma-Aldrich, Wako Pure Chemical Industries and Kanto Chemical and used without further purification. Key compounds were purified by a recycling preparative HPLC (LaboACE LC-5060, Japan Analytical Industry Co., Ltd.) equipped with a gel permeation chromatography (GPC) column (JAIGEL-2HH).

**Nuclear Magnetic Resonance (NMR) Spectroscopy:** NMR spectra were recorded on a JEOL ECS-400 spectrometer and analyzed using an Mnova NMR software. Chemical shifts are presented in parts per million from (ppm) relative to solvent peaks (<sup>1</sup>H NMR: CHCl<sub>3</sub> at 7.26 ppm and <sup>13</sup>C NMR: CDCl<sub>3</sub> at 77.16 ppm).<sup>S1</sup>

**Absorption Spectroscopy:** UV-vis-NIR absorption spectra were recorded on JASCO V-630 and V-670 spectrophotometers using a quartz cuvette for samples in solution and a quartz plate for solid samples. The time course of reactions was recorded with time-interval measurement mode while stirring sample solution at 600 rpm.

**Atomic Force Microscopy (AFM):** AFM measurements were performed on a Bruker Dimension Icon. AFM samples were prepared by spin-coating solutions at the rate of 3000 rpm onto silicon substrates. We carried out measurements at least three points for each sample to ensure reproducibility.

**Fourier-Transform Infrared (FT-IR) Spectroscopy:** FT-IR spectra were acquired on a JASCO FT/IR 4700 spectrophotometer equipped with an attenuated total reflection (ATR)

attachment. The samples were prepared by drying MCH solutions of **NDI2-SC4A** and **NDI1-SC4A** that were cooled from 338 K to 298 K at a rate of 1 K/min. The spectrum of each sample was recorded by 64 scans.

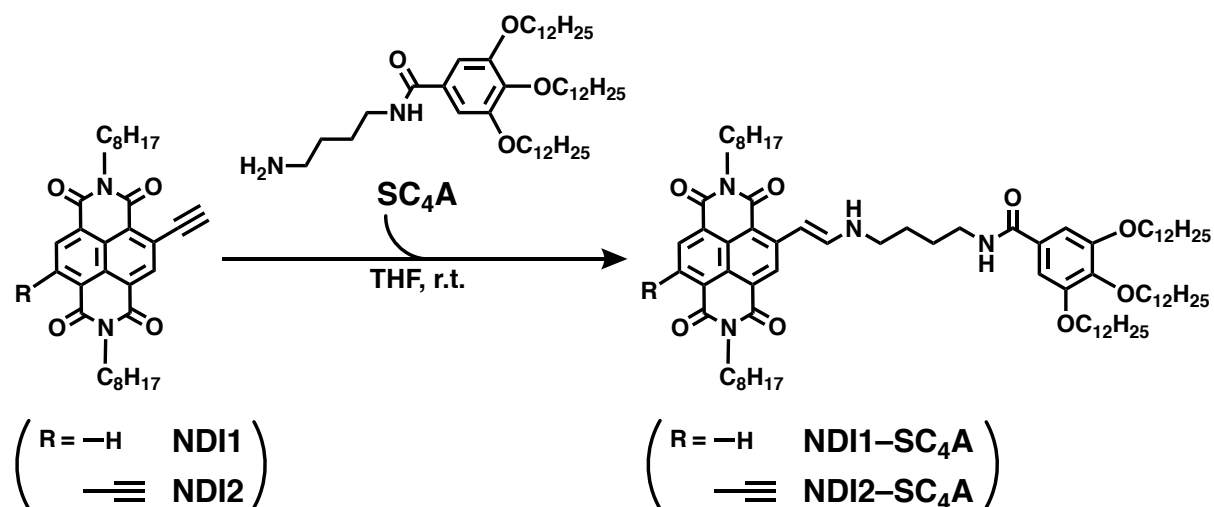
**X-ray Diffraction (XRD) Method:** XRD patterns were recorded on a Rigaku MiniFlex 300 diffractometer equipped with D/teX Ultra X-ray detector. The Cu K $\alpha$  X-ray radiation ( $\lambda = 1.5418 \text{ \AA}$ ) was generated by Cu-rotator anode with operating voltage and current as 40 kV and 15 mA, respectively. The samples were prepared onto non-diffractive silicon plates by drying MCH solutions of **NDI2-SC4A** and **NDI1-SC4A** that were cooled from 338 K to 298 K at a rate of 1 K/min. Data were collected in the range of  $2\theta = 2^\circ$  to  $40^\circ$  with a scan speed of  $2^\circ/\text{min}$  at 298 K.

**Mass Spectrometry:** Matrix-assisted laser desorption/ionization time-of-flight mass spectrometry (MALDI TOF-MS) was conducted with a Shimadzu AXIMA-CFR Plus. Dithranol was used as a matrix. Isotopic distribution pattern was calculated using an iMass 1.6 software.

**Quantum Chemical Calculation:** Computational analysis and graphical representation were carried out with Gaussian 09 software.<sup>S2</sup> Molecular orbitals of optimized structures were obtained by DFT at the  $\omega\text{B97X-D/6-31G}^{**}$  level.

## S2. Synthesis and Characterization

Syntheses of **NDI1**, **NDI2** and **SC4A** were carried out according to the literatures.<sup>S3,S4</sup>

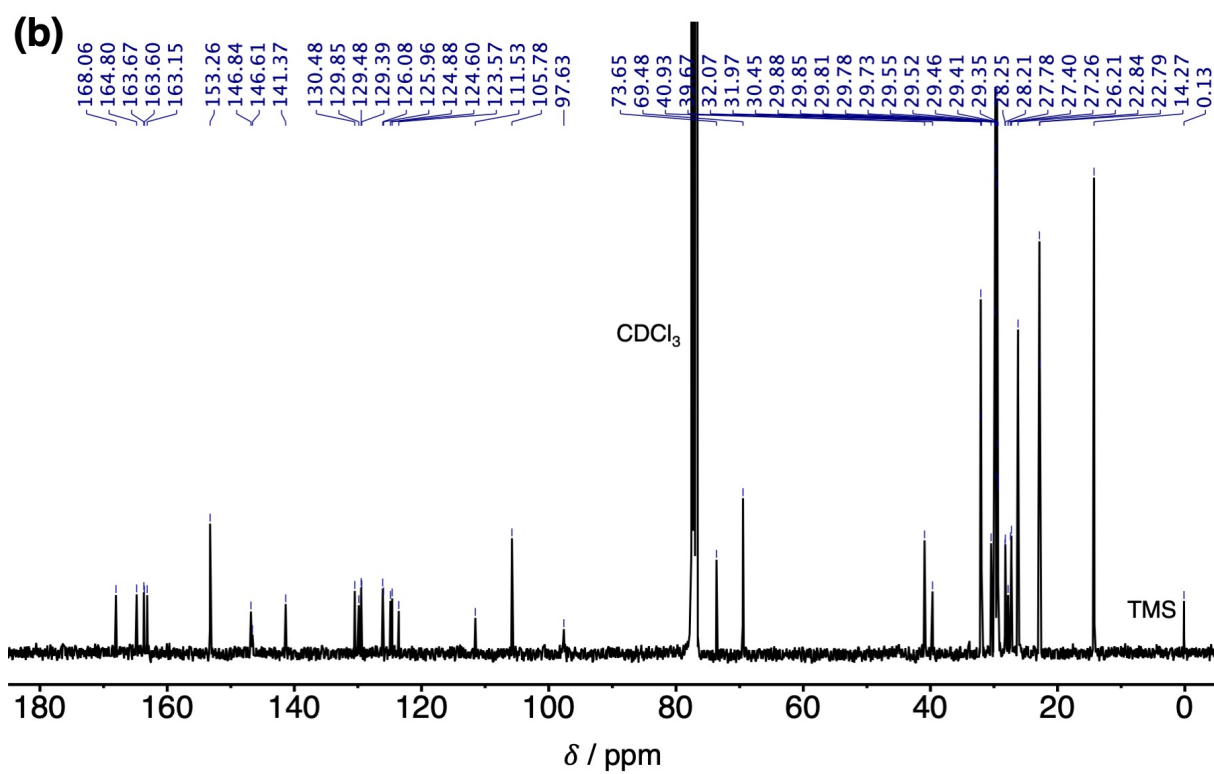
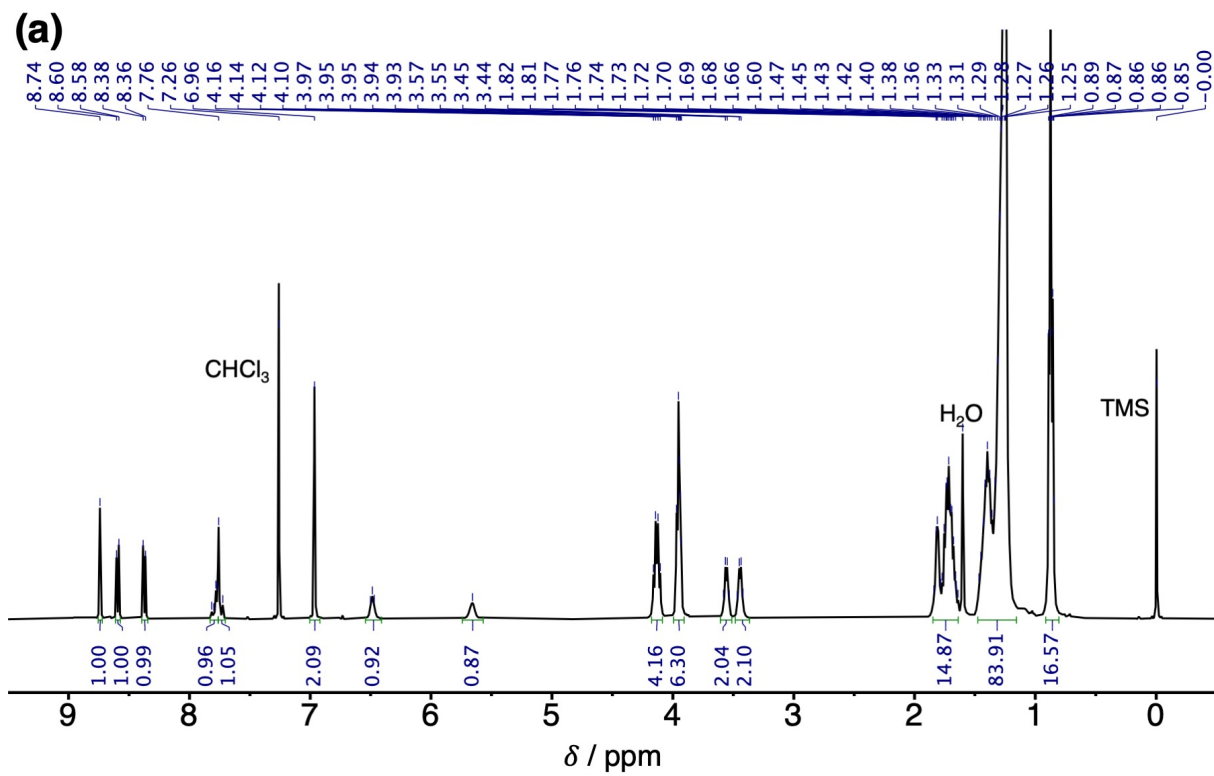


**Synthesis of NDI1-SC<sub>4</sub>A:** In a vial containing **NDI1** (3.9 mg, 7.6  $\mu\text{mol}$ ) and **SC<sub>4</sub>A** (6.9 mg, 9.2  $\mu\text{mol}$ ) were added 1 mL of THF. The reaction mixture was stirred for 29 h under air at room temperature. The resultant product was reprecipitated from  $\text{CHCl}_3$  and MeOH to yield a dark blue solid, **NDI1-SC<sub>4</sub>A** (9.3 mg, 97%). <sup>1</sup>H NMR (400 MHz,  $\text{CDCl}_3$ ):  $\delta$  (ppm) = 0.87 (m, 15H), 1.26 (m, 74H), 1.74 (m, 14H), 3.44 (q,  $J = 6.4$  Hz, 2H), 3.56 (q,  $J = 6.4$  Hz, 2H), 3.95 (m, 6H), 4.13 (q,  $J = 7.3$  Hz, 4H), 5.66 (br, 1H), 6.49 (t,  $J = 6.3$  Hz, 1H), 6.96 (s, 2H), 7.74 (d,  $J = 13.6$  Hz, 1H), 7.79 (m, 1H), 8.37 (d,  $J = 7.8$  Hz, 1H), 8.59 (d,  $J = 7.8$  Hz, 1H), 8.74 (s, 1H). <sup>13</sup>C NMR (101 MHz,  $\text{CDCl}_3$ ):  $\delta$  (ppm) = 14.27, 22.79, 22.84, 26.21, 27.26, 27.40, 27.78, 28.21, 28.25, 29.35, 29.41, 29.46, 29.52, 29.55, 29.73, 29.78, 29.81, 29.85, 29.88, 30.45, 31.97, 32.07, 39.67, 40.93, 69.48, 73.65, 97.63, 105.78, 111.53, 123.57, 124.60, 124.88, 125.96, 126.08, 129.39, 129.48, 129.85, 130.48, 141.37, 146.61, 146.84, 153.26, 163.15, 163.60, 163.67, 164.80, 168.06. MALDI TOF-MS (positive ion, reflectron mode):  $m/z$  calcd. for  $\text{C}_{79}\text{H}_{126}\text{N}_4\text{O}_8$   $[\text{M}]^+$  1258.96; found: 1258.65.

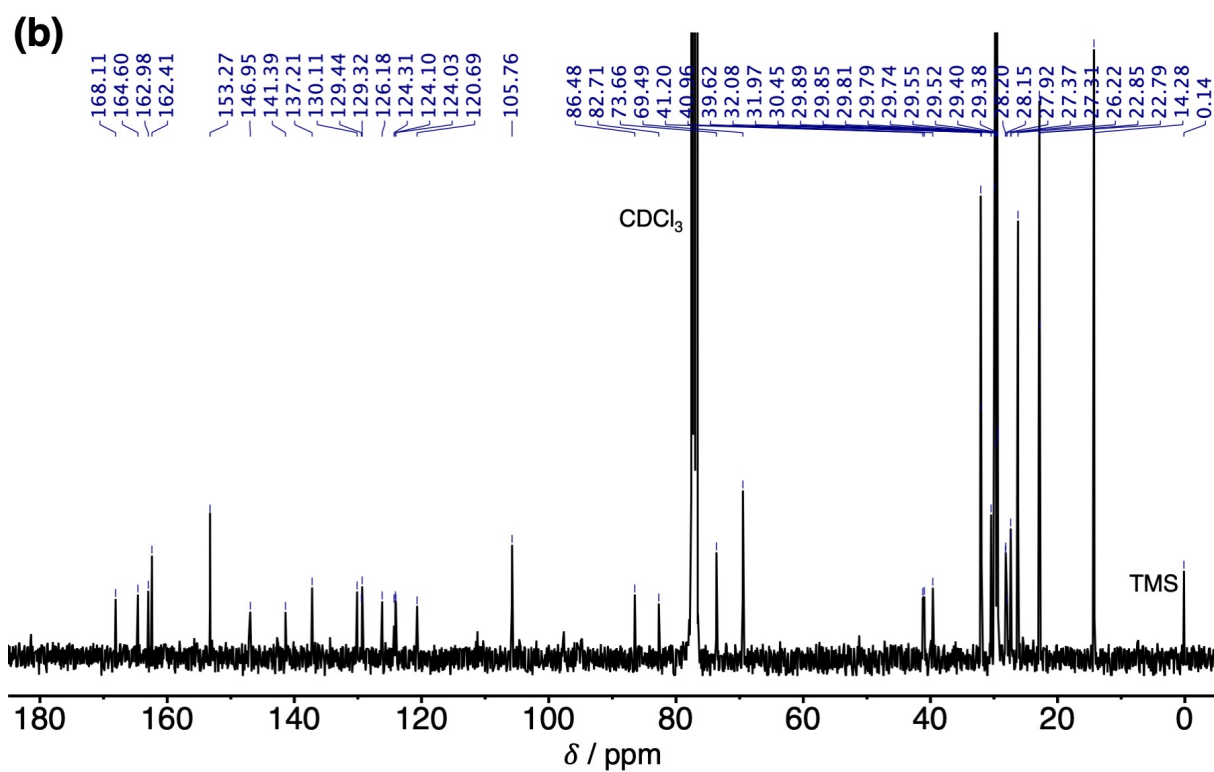
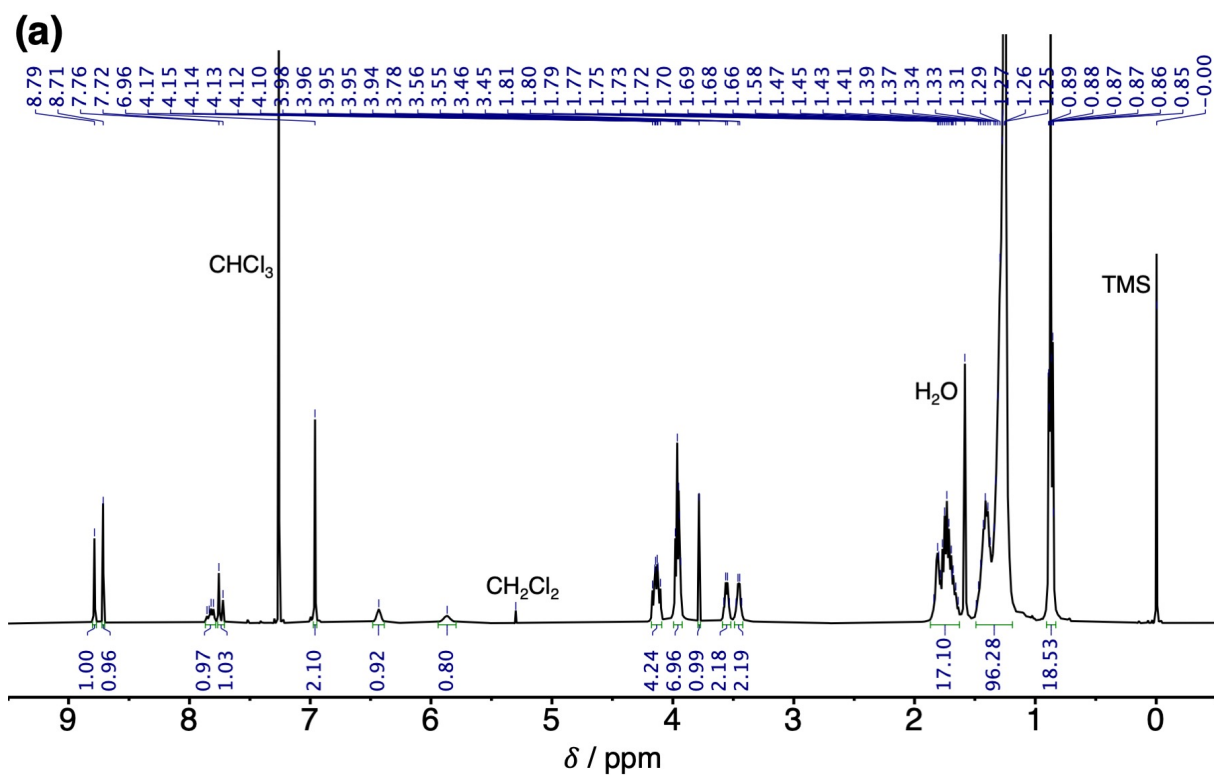
**Synthesis of NDI2-SC<sub>4</sub>A:** In a vial containing **NDI2** (3.1 mg, 5.8  $\mu\text{mol}$ ) and **SC<sub>4</sub>A** (5.4 mg, 7.3  $\mu\text{mol}$ ) were added 1 mL of THF. The reaction mixture was stirred for 28 h under air at room temperature. The resultant product was reprecipitated from  $\text{CHCl}_3$  and MeOH to yield a dark blue solid, **NDI2-SC<sub>4</sub>A** (7.0 mg, 94%). <sup>1</sup>H NMR (400 MHz,  $\text{CDCl}_3$ ):  $\delta$  (ppm) = 0.87 (m, 15H), 1.26 (m, 74H), 1.74 (m, 14H), 3.45 (q,  $J = 6.4$  Hz, 2H), 3.56 (q,  $J = 6.3$  Hz, 2H), 3.78 (s, 1H), 3.96 (m, 6H), 4.14 (m, 4H), 5.87 (br, 1H), 6.43 (br, 1H), 6.96 (s, 2H), 7.74 (d,  $J = 13.6$  Hz, 1H), 7.83 (dd,  $J = 13.7$  Hz, 7.4 Hz, 1H), 8.71 (s, 1H), 8.79 (s, 1H). <sup>13</sup>C NMR (101 MHz,

CDCl<sub>3</sub>):  $\delta$  (ppm) = 14.28, 22.79, 22.85, 26.22, 27.31, 27.37, 27.92, 28.15, 28.20, 29.38, 29.40, 29.52, 29.55, 29.74, 29.79, 29.81, 29.85, 29.89, 30.45, 31.97, 32.08, 39.62, 40.96, 41.20, 69.49, 73.66, 82.71, 86.48, 105.76, 120.69, 124.03, 124.10, 124.31, 126.18, 129.32, 129.44, 130.11, 137.21, 141.39, 146.95, 153.27, 162.41, 162.98, 164.60, 168.11. MALDI TOF–MS (positive ion, reflectron mode):  $m/z$  calcd. for C<sub>81</sub>H<sub>126</sub>N<sub>4</sub>O<sub>8</sub> [M]<sup>+</sup> 1282.96; found: 1283.21.

Note that, in the case of **NDI2**, the corresponding amine bisadduct was not formed under these conditions, because the second amine-addition reaction is much slower than the initial one owing to the less electron-accepting ability of the amine monoadduct than that of **NDI2**.



(a) <sup>1</sup>H NMR and (b) <sup>13</sup>C NMR spectra of NDI1-SC<sub>4</sub>A in CDCl<sub>3</sub> at 298 K.



(a)  $^1\text{H}$  NMR and (b)  $^{13}\text{C}$  NMR spectra of NDI2-SC<sub>4</sub>A in  $\text{CDCl}_3$  at 298 K.

### S3. Spectral Analyses

**Analysis of Cooperative (i.e., Nucleation–Elongation) Process:**<sup>S5</sup> The degree of aggregation ( $\alpha_{\text{agg}}$ ) of **NDI2–SC4A** was calculated by eqn (S1);

$$\alpha_{\text{agg}} \approx (A - A_{\text{mono}}) / (A_{\text{agg}} - A_{\text{mono}}) \quad (\text{S1})$$

where  $A$  is the absorbance at 725 nm,  $A_{\text{mono}}$  is the absorbance of the **NDI2–SC4A** monomer obtained from the absorbance at 725 nm at 338 K (= 0.01) and  $A_{\text{agg}}$  is the absorbance of the **NDI2–SC4A** supramolecular assemblies obtained from the absorbance at 725 nm at 277 K (= 0.22). The elongation process of supramolecular assemblies can be expressed by eqn (S2);

$$\alpha_{\text{agg}} = \alpha_{\text{SAT}} [1 - \exp(-\Delta H_e (T - T_e) / RT_e^2)] \quad (\text{S2})$$

where  $\Delta H_e$  is an elongation enthalpy,  $R$  is the ideal gas constant,  $T_e$  is the critical elongation temperature,  $T$  is the absolute temperature and  $\alpha_{\text{SAT}}$  is the constant used to ensure that  $\alpha_{\text{agg}}/\alpha_{\text{SAT}}$  does not exceed unity. The plot of  $\alpha_{\text{agg}}$  versus temperature of **NDI2–SC4A** can be fitted well by eqn (S2) to afford  $\Delta H_e$  and  $T_e$ . See Table S1 and Fig. S1.

**Kinetic Analysis:** The hydroamination reaction rate of **NDI2** in the presence of excess amine (**SC4A**) can be calculated by using eqn (S3) and eqn (S4):

$$d[\text{NDI2–SC4A}]/dt = k_{\text{obs}} \{[\text{NDI2}]_0 - [\text{NDI2–SC4A}]\} \quad (\text{S3})$$

$$[\text{NDI2–SC4A}] = [\text{NDI2}]_0 \{1 - \exp(-k_{\text{obs}}t)\} \quad (\text{S4})$$

where  $k_{\text{obs}}$  (in  $\text{s}^{-1}$ ) is a pseudo-first order rate constant for the formation of the amine monoadduct (**NDI2–SC4A**), and  $[\text{NDI2}]_0$  is the initial concentration of **NDI2**. In case of time-interval UV–vis absorption measurements, the absorbance at 416 nm ( $A_{416}$ ) is the sum of absorption due to **NDI2**, **NDI2–SC4A** and its assemblies. Given that the absorption coefficients of **NDI2–SC4A** and its assemblies at 416 nm are comparable, the time course of  $A_{416}$  is given by eqn (S5):

$$A_{416} = \varepsilon_{\text{NDI2}}[\text{NDI2}]_0 \{\exp(-k_{\text{obs}}t)\} + \varepsilon_{\text{NDI2–SC4A}}[\text{NDI2}]_0 \{1 - \exp(-k_{\text{obs}}t)\} \quad (\text{S5})$$

where  $\varepsilon_{\text{NDI2}}$  and  $\varepsilon_{\text{NDI2–SC4A}}$  are the molar extinction coefficients of **NDI2** and the sum of **NDI2–SC4A** and its assemblies, respectively. The above description can be also applied to **NDI1**.

#### S4. Supporting Data

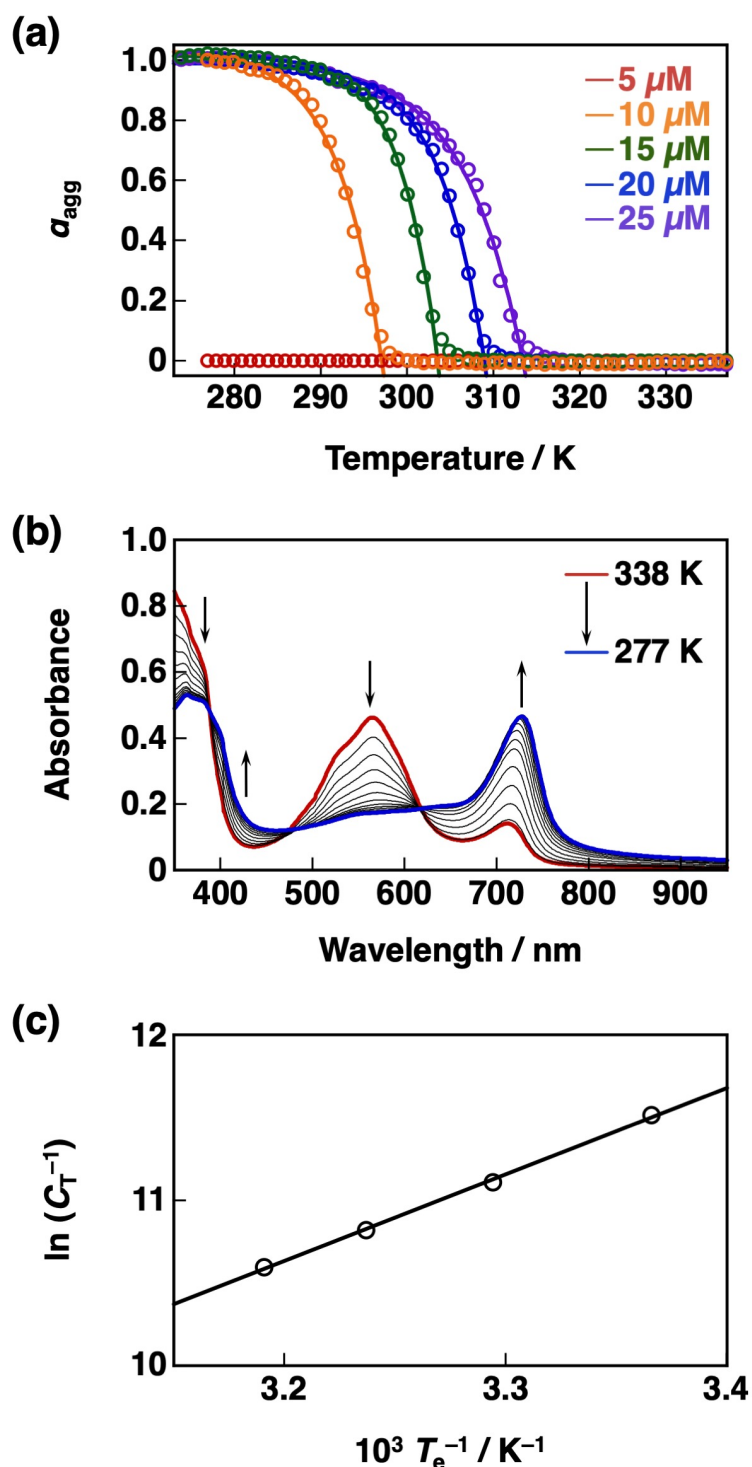


**Fig. S1** (a) Plots of  $\alpha_{agg}$  of ND12-SC4A calculated from the absorbance change at 725 nm versus temperature observed in the cooling process from 338 K to 277 K (1 K/min) at different total concentrations ( $C_T$ ) in MCH. The solid lines are fitting curves by a cooperative model with  $R^2$  values over 0.99. (b) UV-vis-NIR absorption spectral changes of ND12-SC4A (40  $\mu\text{M}$ ) in MCH upon cooling from 338 K (red line) to 277 K (blue line) at a rate of 1 K/min.

(c) A van't Hoff plot ( $\ln C_T^{-1}$  as a function of  $T_e^{-1}$ ) showing a linear relationship with an  $R^2$  value of 0.999. The standard enthalpy ( $\Delta H^\circ$ ) was obtained to be  $-43.5 \text{ kJ mol}^{-1}$ .

**Table S1** Thermodynamic parameters ( $\alpha_{\text{SAT}}$ ,  $T_e$ ,  $\Delta H_e$ ) obtained by fitting curves with a cooperative model at different  $C_T$  in Fig. S1a

$C_T / \mu\text{M}$	$\alpha_{\text{SAT}}$	$T_e / \text{K}$	$\Delta H_e / \text{kJ mol}^{-1}$
10	1.038	297.1	-140.1
15	1.014	303.6	-176.6
20	0.990	308.9	-153.1
25	0.999	313.4	-118.5

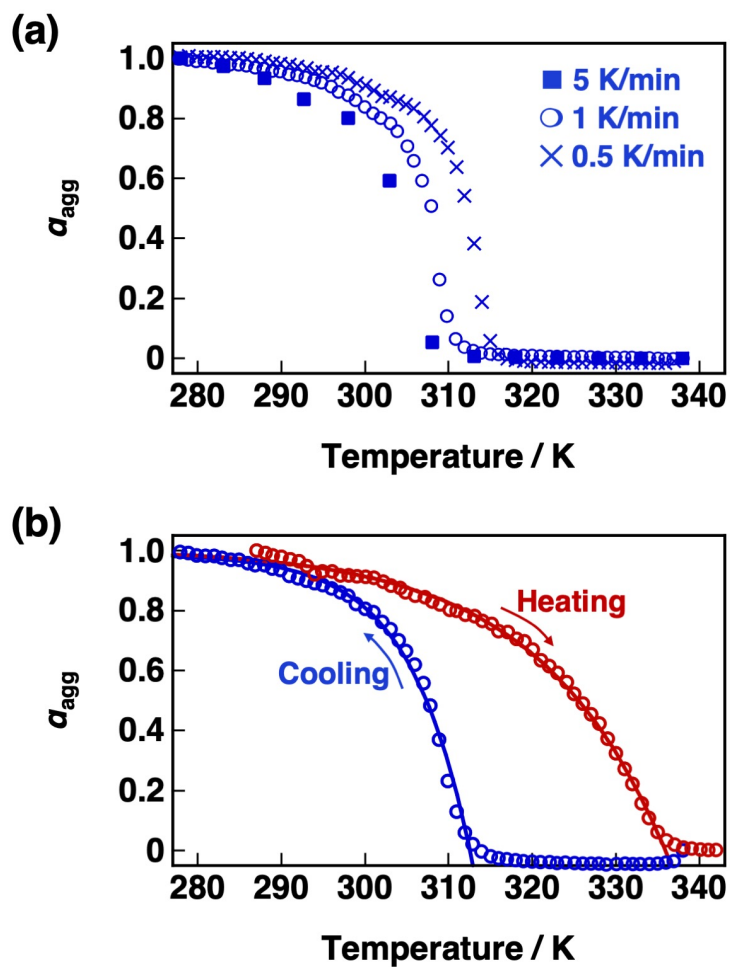


**Fig. S2** (a) Effect of cooling rates on the aggregation processes of NDI2-SC4A ( $C_T = 25 \mu\text{M}$ ) in MCH. (b) The plot of  $\alpha_{agg}$  of NDI2-SC4A calculated from the absorbance at 725 nm versus temperature observed in the cooling (blue) and heating (red) processes in MCH at a rate of 1 K/min.

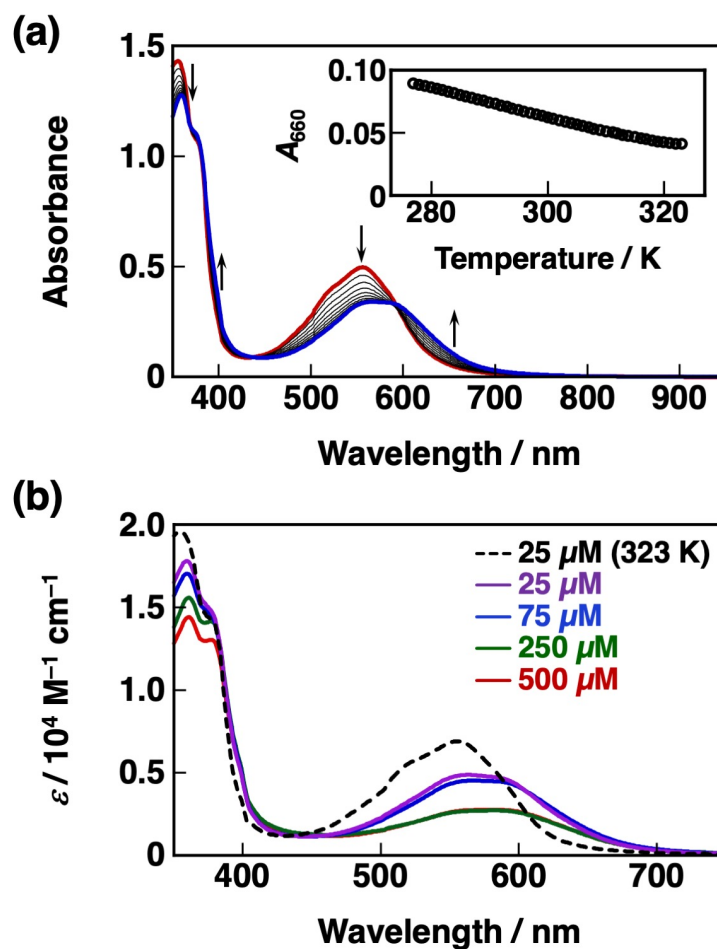


**Fig. S3** (a) UV-vis-NIR absorption spectral changes of NDI1-SC<sub>4</sub>A (75  $\mu\text{M}$ ) in MCH upon cooling from 323 K (red line) to 277 K (blue line) at a rate of 1 K/min. Inset shows the plot of absorbance change at 660 nm versus temperature. (b) Comparison of UV-vis-NIR absorption spectra of NDI1-SC<sub>4</sub>A at different concentrations in MCH upon cooling to 277 K.

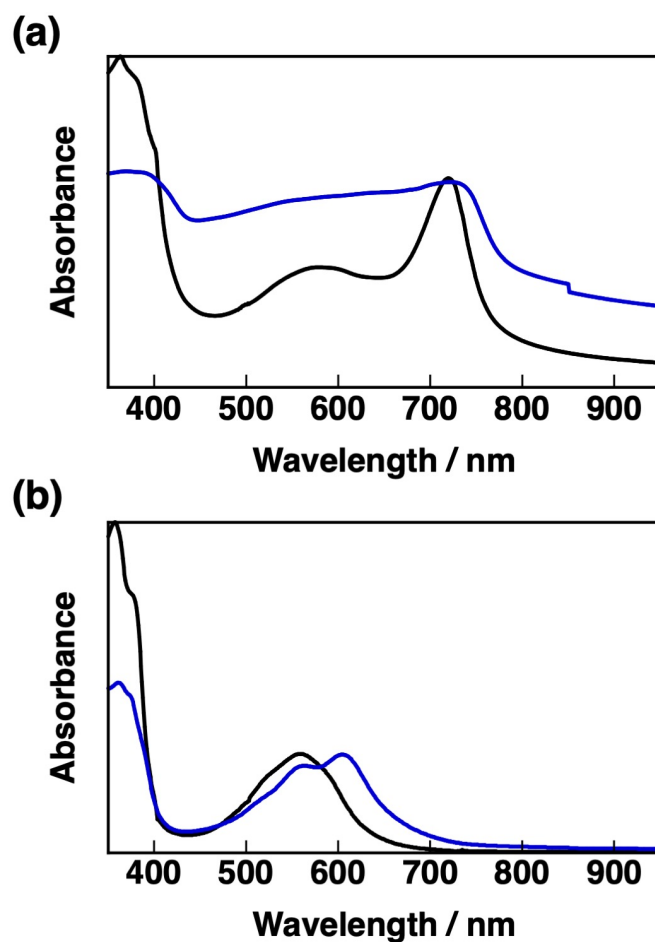


**Fig. S4** Comparison of UV-vis-NIR absorption spectra of the supramolecular polymers of (a) **NDI2-SC<sub>4</sub>A** and (b) **NDI1-SC<sub>4</sub>A** in the MCH solutions (black lines) and in the solid states (blue lines). The UV-vis-NIR absorption spectrum of **NDI2-SC<sub>4</sub>A** in the solid state exhibited the absorption band at 726 nm, which was nearly identical to that of the supramolecular assembly in MCH. This result indicates that the dried sample retained its supramolecular structure.

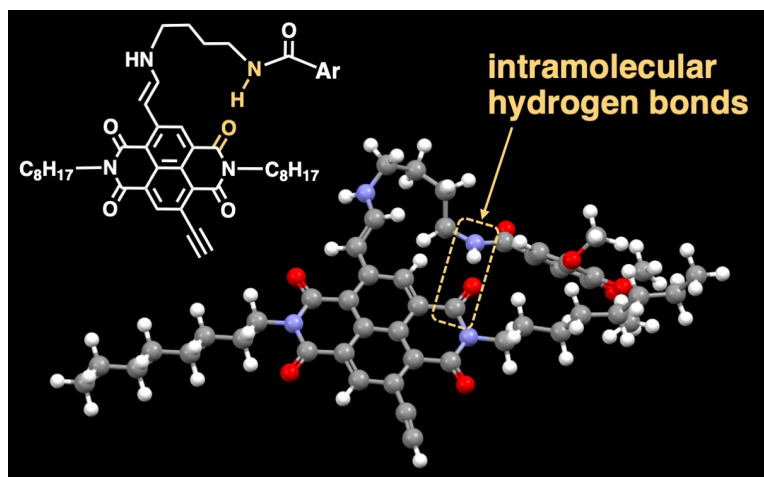


**Fig. S5** Optimized structure of NDI2-SC<sub>4</sub>A that forms an intramolecular hydrogen bond between the amide hydrogen and the imide carbonyl oxygen, calculated at the  $\omega$ B97X-D/6-31G\*\* level. The alkoxy groups ( $-\text{OC}_{12}\text{H}_{25}$ ) were substituted by methoxy group for simplicity. Atom colour code: grey, C; red, O; blue, N; white, H.

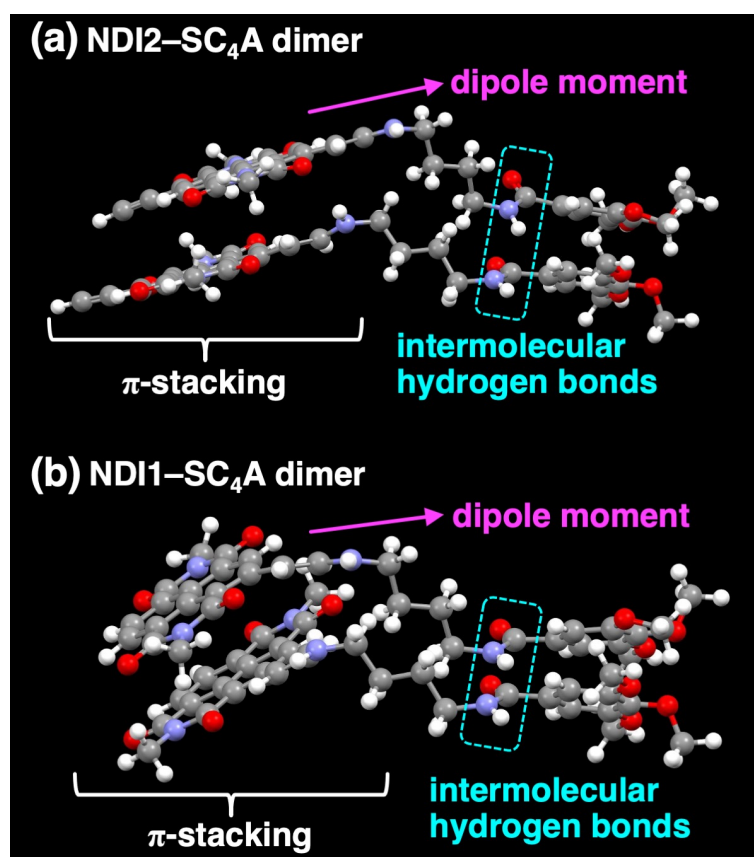


**Fig. S6** Optimized structures of (a) **NDI2-SC<sub>4</sub>A** dimer and (b) **NDI1-SC<sub>4</sub>A** dimer calculated at the  $\omega$ B97X-D/6-31G\*\* level. The alkoxy groups ( $-\text{OC}_{12}\text{H}_{25}$ ) and octyl groups ( $-\text{C}_8\text{H}_{17}$ ) were substituted by methoxy group and methyl group for simplicity. Atom colour code: grey, C; red, O; blue, N; white, H. The center-to-center distances between the NDI  $\pi$ -planes in **NDI2-SC<sub>4</sub>A** dimer and **NDI1-SC<sub>4</sub>A** are 0.44 nm and 0.35 nm, respectively. Such  $\pi$ -stacking structures should also be found in the supramolecular assemblies of **NDI2-SC<sub>4</sub>A** and **NDI1-SC<sub>4</sub>A**. However, the XRD peaks attributed to these  $\pi$ -stacking structures ( $2\theta \sim 20.2^\circ$  for the **NDI2-SC<sub>4</sub>A** assembly and  $25.4^\circ$  for the **NDI1-SC<sub>4</sub>A** assembly) were overlapped with the broad alkyl halo peaks (Fig. S7), which precluded a more detailed analysis.

**Table S2** Dipole moments of **NDI2-SC<sub>4</sub>A**, **NDI1-SC<sub>4</sub>A** and their dimers obtained by DFT calculation at the  $\omega$ B97X-D/6-31G\*\* level.

Compound	Dipole moment / D
<b>NDI2-SC<sub>4</sub>A</b>	9.2
<b>NDI2-SC<sub>4</sub>A dimer</b>	13.1
<b>NDI1-SC<sub>4</sub>A</b>	9.2
<b>NDI1-SC<sub>4</sub>A dimer</b>	14.9

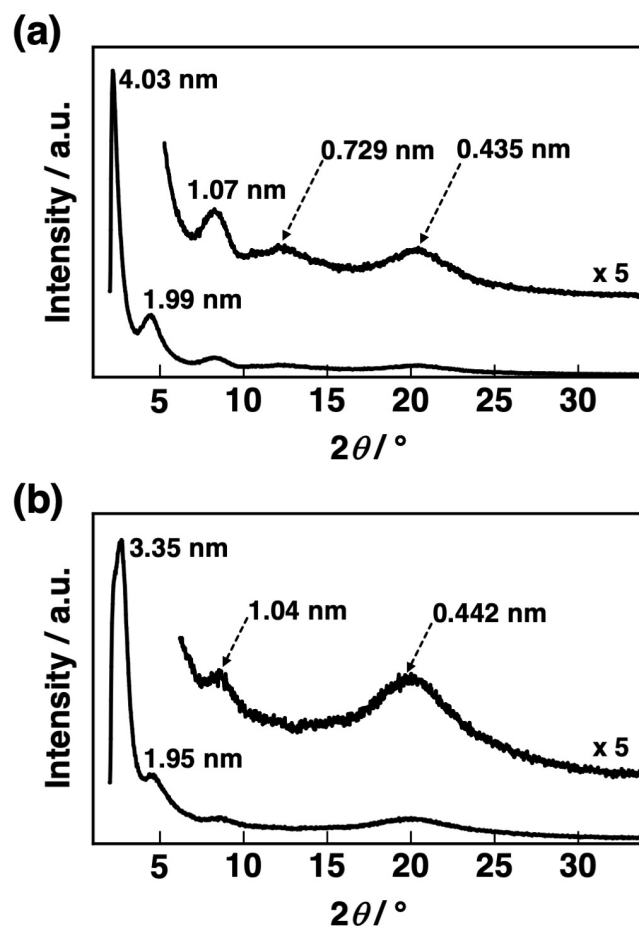


**Fig. S7** XRD patterns of the supramolecular assemblies of (a) NDI2-SC4A and (b) NDI1-SC4A in the solid states at 298 K. The background (non-diffractive silicon sample plate) data were subtracted from the raw data.

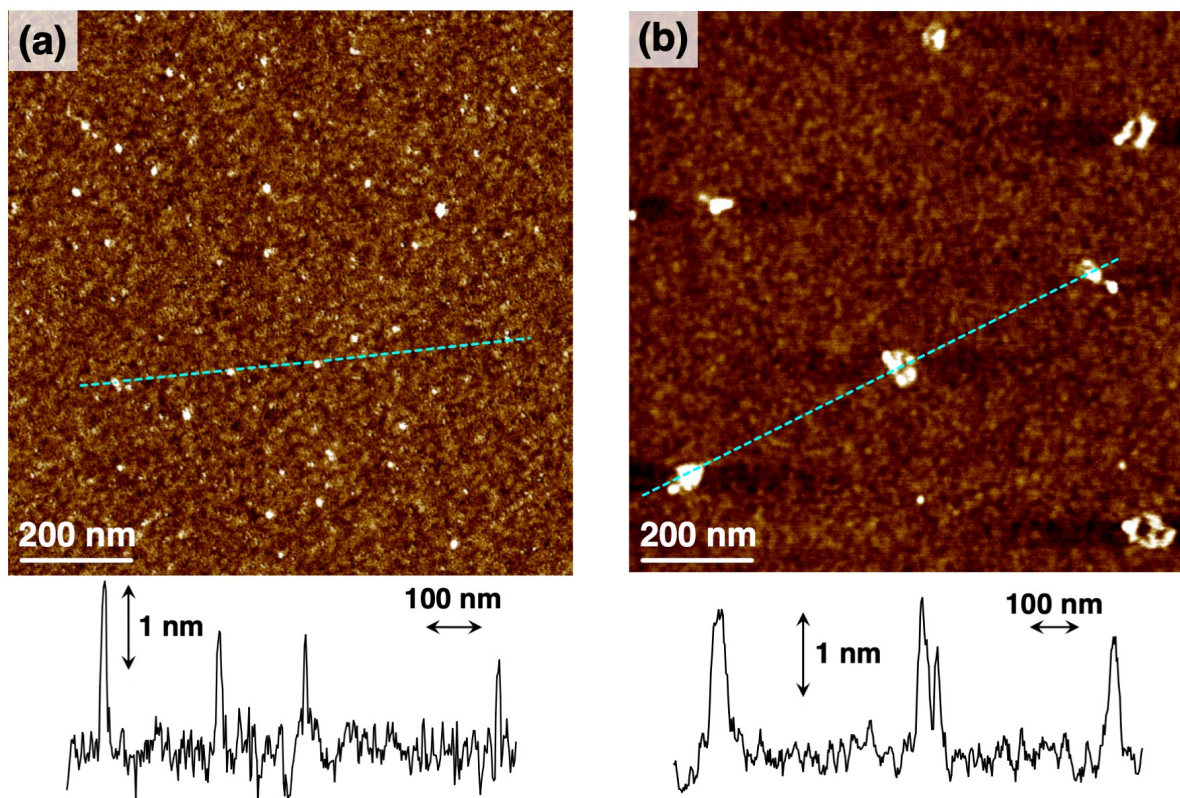


**Fig. S8** AFM images of the supramolecular assemblies of (a) **NDI2-SC<sub>4</sub>A** and (b) **NDI1-SC<sub>4</sub>A**. The height profiles of the cross-section (cyan dashed lines) are also shown. The AFM samples were prepared by spin-coating from the MCH solutions of **NDI2-SC<sub>4</sub>A** (25  $\mu$ M) and **NDI1-SC<sub>4</sub>A** (25  $\mu$ M). The average height of **NDI2-SC<sub>4</sub>A** supramolecular assemblies is *ca.* 1.5 nm, suggesting the face-on orientation of several **NDI2-SC<sub>4</sub>A** molecules with the  $\pi$ -plane parallel to the substrate.

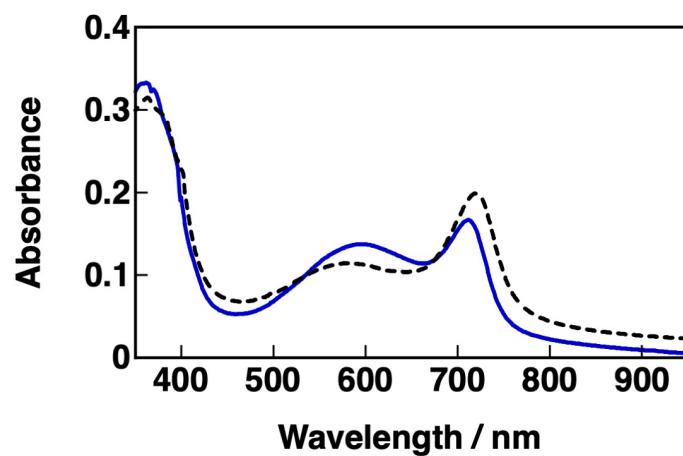


**Fig. S9** UV-vis-NIR absorption spectrum at 4000 min after the start of the reaction between **NDI2** (25  $\mu\text{M}$ ) and **SC<sub>4</sub>A** (blue solid line) and that of the **NDI2-SC<sub>4</sub>A** supramolecular assemblies ( $C_{\text{T}} = 25 \mu\text{M}$ ) in MCH at 298 K.

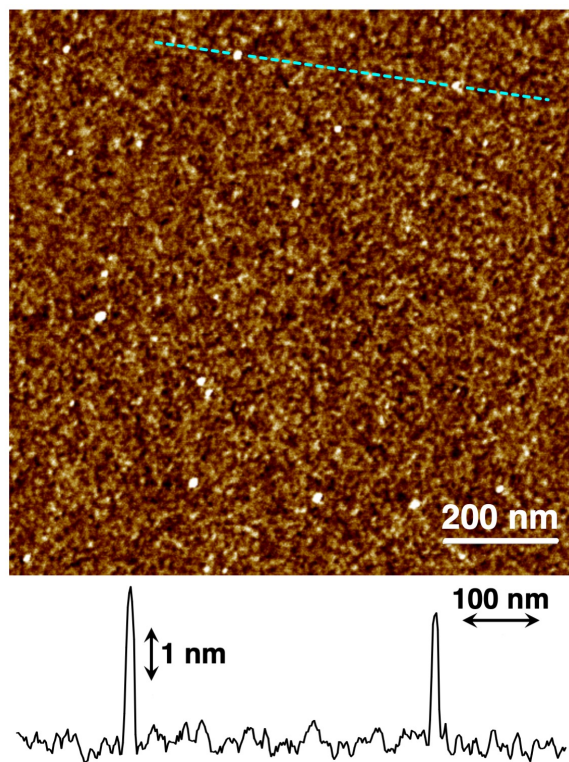


**Fig. S10** AFM image at 3983 min after the start of the reaction between **NDI2** (25  $\mu\text{M}$ ) and **SC<sub>4</sub>A** (100  $\mu\text{M}$ ). The height profile of the cross-section (cyan dashed line) is also shown.

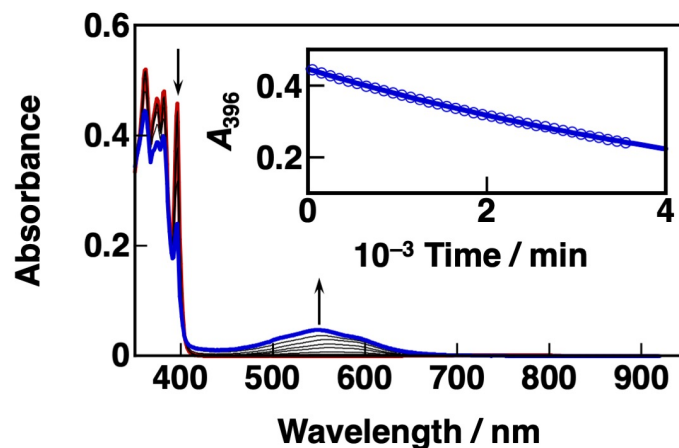


**Fig. S11** UV-vis-NIR absorption spectral changes of **NDI1** (25  $\mu\text{M}$ ) observed upon addition of **SC4A** (100  $\mu\text{M}$ ) in MCH at 298 K. The absorbance at 396 nm due to the  $\pi\text{-}\pi^*$  transition of **NDI1** decreased and a charge-transfer band appeared at 555 nm, following a typical first order kinetic equation under this pseudo-first order conditions. No distinct absorption bands due to the formation of the **NDI1-SC4A** supramolecular assemblies were observed, unlike in the case of **NDI2-SC4A**. Inset shows the time profile of the absorbance at 396 nm (blue circle), fitted to a first order kinetic curve with an  $R^2$  value of 0.999. The pseudo-first order and second order rate constants were determined to be  $2.7 \times 10^{-6} \text{ s}^{-1}$  and  $2.7 \times 10^{-2} \text{ M}^{-1} \text{ s}^{-1}$ , respectively. Note that we tried to see where the reaction was completed by extending the reaction time, but it took over  $1.6 \times 10^4 \text{ min}$  (270 h) to reach 90% completion of the reaction, and the time-course UV-vis-NIR absorption spectra could not be fully obtained due to the stability issues with the compounds and the instrumental settings.

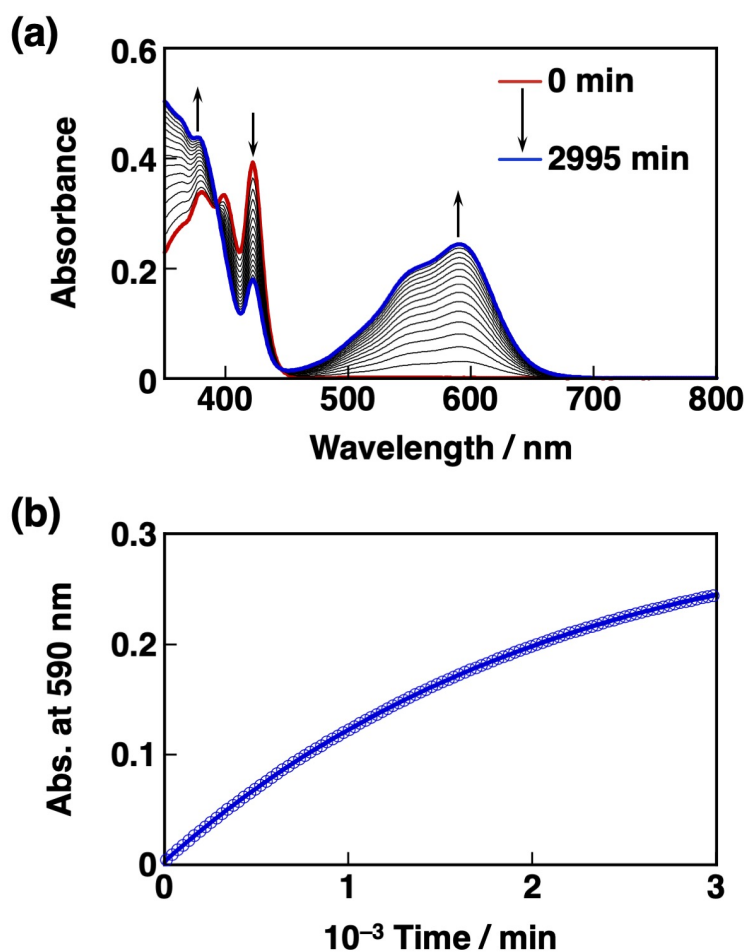


**Fig. S12** (a) UV-vis-NIR absorption spectral changes of **NDI2** (25  $\mu\text{M}$ ) observed upon addition of **SC<sub>4</sub>A** (100  $\mu\text{M}$ ) in toluene at 298 K. (b) Time profile of the absorbance at 590 nm (blue circle), fitted by a first order kinetic curve under this pseudo-first order conditions ( $R^2$  value > 0.999). The pseudo-first order and second order rate constants were determined to be  $7.74 \times 10^{-6} \text{ s}^{-1}$  and  $7.74 \times 10^{-2} \text{ M}^{-1} \text{ s}^{-1}$ , respectively.

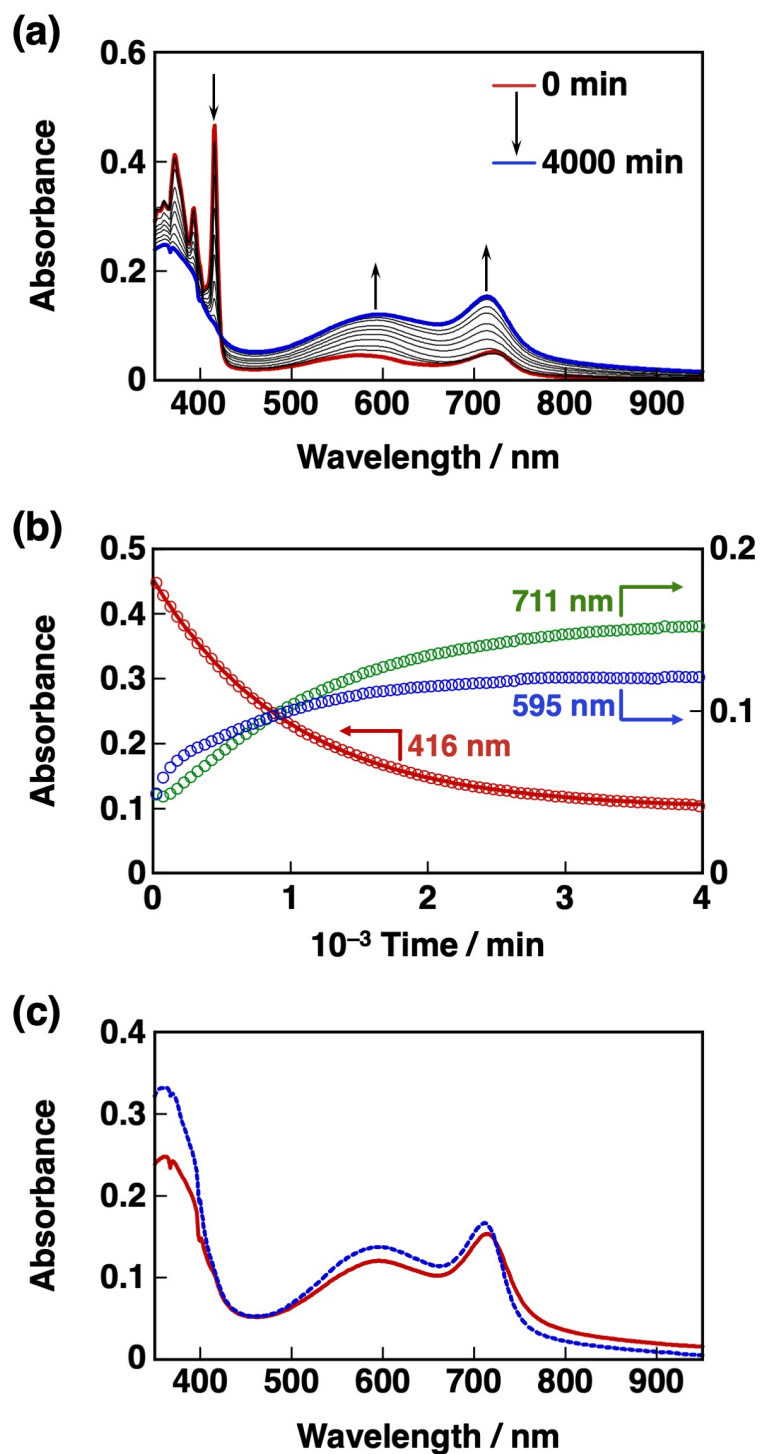


**Fig. S13** (a) UV-vis-NIR absorption spectral changes of NDI2 (15  $\mu\text{M}$ ) observed upon addition of SC4A (100  $\mu\text{M}$ ) in the presence of the supramolecular assemblies of NDI2-SC4A (10  $\mu\text{M}$ ) as seeds in MCH at 298 K.<sup>S6</sup> (b) Time profiles of the absorbance at 416 nm (red circle), 595 nm (blue circle) and 711 nm (green circle) during the reaction. The decay of the absorbance at 416 nm was fitted by a first order kinetic curve under this pseudo-first order conditions ( $R^2$  value > 0.999). (c) Comparison of the UV-vis-NIR absorption spectrum after the reaction in the absence (blue dashed line) and the presence (red line) of the seed.

## S5. Supporting References

- S1. G. R. Fulmer, A. J. M. Miller, N. H. Sherden, H. E. Gottlieb, A. Nudelman, B. M. Stoltz, J. E. Bercaw and K. I. Goldberg, *Organometallics*, 2010, **29**, 2176.
- S2. Gaussian 09, Revision E.01, M. J. Frisch, G. W. Trucks, H. B. Schlegel, G. E. Scuseria, M. A. Robb, J. R. Cheeseman, G. Scalmani, V. Barone, B. Mennucci, G. A. Petersson, H. Nakatsuji, M. Caricato, X. Li, H. P. Hratchian, A. F. Izmaylov, J. Bloino, G. Zheng, J. L. Sonnenberg, M. Hada, M. Ehara, K. Toyota, R. Fukuda, J. Hasegawa, M. Ishida, T. Nakajima, Y. Honda, O. Kitao, H. Nakai, T. Vreven, J. A. Montgomery, Jr., J. E. Peralta, F. Ogliaro, M. Bearpark, J. J. Heyd, E. Brothers, K. N. Kudin, V. N. Staroverov, R. Kobayashi, J. Normand, K. Raghavachari, A. Rendell, J. C. Burant, S. S. Iyengar, J. Tomasi, M. Cossi, N. Rega, J. M. Millam, M. Klene, J. E. Knox, J. B. Cross, V. Bakken, C. Adamo, J. Jaramillo, R. Gomperts, R. E. Stratmann, O. Yazyev, A. J. Austin, R. Cammi, C. Pomelli, J. W. Ochterski, R. L. Martin, K. Morokuma, V. G. Zakrzewski, G. A. Voth, P. Salvador, J. J. Dannenberg, S. Dapprich, A. D. Daniels, Ö. Farkas, J. B. Foresman, J. V. Ortiz, J. Cioslowski, and D. J. Fox, Gaussian, Inc., Wallingford CT, 2009.
- S3. A. Takai and M. Takeuchi, *Bull. Chem. Soc. Jpn.*, 2018, **91**, 44.
- S4. S. Ogi, V. Stepanenko, J. Theirs and F. Würthner, *J. Am. Chem. Soc.*, 2016, **138**, 670.
- S5. S. Ogi, V. Stepanenko, K. Sugiyasu, M. Takeuchi and F. Würthner, *J. Am. Chem. Soc.*, 2015, **137**, 3300.
- S6. Experimental details: A MCH solution of **NDI2-SC4A** (25  $\mu$ M) was cooled from 338 K to 298 K at the rate of 1 K/min. Separately, a MCH solution of **NDI2** (25  $\mu$ M) was also prepared. These two solutions were then mixed in a 2:3 ratio at 298 K to afford a MCH solution (3 mL) containing the supramolecular assemblies of **NDI2-SC4A** (10  $\mu$ M) and **NDI2** (15  $\mu$ M). The supramolecular assemblies of **NDI2-SC4A** can be regarded as seeds, because the critical elongation temperature of **NDI2-SC4A** at 10  $\mu$ M is 297 K (Table S1). Next, **SC4A** (100  $\mu$ M) was added to the MCH solution while stirring at 600 rpm to initiate the amino-yne click reaction.